*Materials Research*. 2025; 28(suppl. 1): e20250117
DOI: https://doi.org/10.1590/1980-5373-MR-2025-0117



# Micrometric and Nanometric Characterization of Rock Aggregates Using AIMS, AFM, and SEM to Further Discussions on Geotechnical Roughness Classification Systems

***Haline Dugolin Ceccato*[a], *Augusto Gonçalves Nobre*[b,c*], *Andréa Valli Nummer*[b], *Rinaldo José Barbosa Pinheiro*[a], *Ricardo Barreto da Silva*[d], *Josué Neroti Rigue*[d]**

[a]*Universidade Federal de Santa Maria (UFSM), Departamento de Transportes, Santa Maria, RS, Brasil.*
[b]*Universidade Federal de Santa Maria (UFSM), Departamento de Geociências, Santa Maria, RS, Brasil.*
[c]*Universidade de Brasília (UNB), Intituto de Geociências, Brasília, DF, Brasil.*
[d]*Universidade Federal de Santa Maria (UFSM), Departamento de Física, Santa Maria, RS, Brasil.*

Received: January 10, 2025; Revised: April 13, 2025; Accepted: June 01, 2025

The characterization of surface roughness in rock aggregates is essential for geotechnical engineering, directly influencing pavement performance and durability. This study compared three roughness analysis techniques: the Aggregate Imaging Measurement System (AIMS), Atomic Force Microscopy (AFM), and Scanning Electron Microscopy (SEM). Samples of volcanic rock (SUL) and plutonic rock (MIN) were analysed using all three techniques, revealing discrepancies in the results. AIMS presented limitations in representing materials with micrometric roughness and substantially coarse grain sizes, such as the MIN aggregate, where dominant minerals influenced the texture due to wavelet processing. AFM proved to be an efficient roughness characterization technique, quantifying parameters such as average roughness (Ra), root mean square roughness (Rq), surface skewness (Rsk), and surface kurtosis (Rku), but was limited to small scanning areas. The results reveal potential inconsistencies in traditional classification systems, particularly their inability to detect variations in rocks with different textures and granulometries. Data obtained from AFM and SEM demonstrated greater sensitivity, revealing features not identified by AIMS, especially in fine-grained materials like the SUL rock. Therefore, integrating micro- and nanoscale analyses is proposed as a complementary approach to overcome the limitations of conventional methods.

**Keywords:** *Surface roughness, Pavement engineering, Aggregate characterization, Atomic Force Microscopy, Aggregate Imaging Measurement System, Morphological analysis methods.*

## 1. Introduction

Aggregates play a central role in civil engineering, being fundamental components in asphalt mixtures and cementitious concretes, where they represent the largest proportion of the material's total volume[1]. The morphological properties of aggregates, including shape, texture, and size, directly influence the structural and functional performance of these materials[2]. The geometric complexity resulting from these characteristics significantly impacts structural strength, stability, and the ability to organise asphalt mixtures, aspects crucial for durability and efficiency in applications such as pavement and concrete structures[3,4]. Among morphological parameters, the textural relationships of crystals and, particularly, the roughness of aggregates, play a determining role in wear resistance, adhesion to binders, and moisture susceptibility[5]. Aggregates with angular and rough surfaces are associated with higher binder adhesion and mechanical stability, while smoother surfaces favors void distribution, directly influencing structural and functional performance[6]. In this context, the development and application of robust and precise morphological characterization methods are essential for predicting the mechanical behaviour of asphalt mixtures and concretes[7,8].

Traditionally, aggregate morphological characterization involves analytical laboratory techniques that, although widely used, are often time-consuming, subjective, and operator-dependent[9,10]. The introduction of digital image analysis tools, such as the Aggregate Imaging Measurement System (AIMS), revolutionized this field by offering efficiency and objectivity in classification. However, AIMS has notable limitations, such as restriction to the bulk scale and difficulty in accurately distinguishing texture, angularity, granulometry and shape properties[11-14]. As AIMS relies on image acquisition through a fixed camera with automatic focus[15], the images generated are not always representative of the aggregate. Consequently, given the inadequacy of the image dataset, the wavelet-based processing used to obtain roughness is compromised.

Given these limitations, advanced microscopy techniques, such as Atomic Force Microscopy (AFM), emerge as promising alternatives for evaluating rock aggregate morphology[16-18]. AFM enables topographic characterization at micro- and nanoscale, providing quantitative measurements of surface roughness with high resolution[19,20].This technique can identify morphological

*e-mail: augusto.goncalves@unb.br
**Associate Editor**: Eliana Muccillo.
**Editor-in-Chief**: Luiz Antonio Pessan.

variations in extremely small regions, with resolutions below 200 nm, and is also a non-destructive method capable of generating precise three-dimensional (3D) profiles[21-27]. AFM has emerged as a prominent characterization method at micro- and nanoscale across various scientific domains, including biology, physics, chemistry, and materials science[28-31]. Its efficiency in evaluating the morphology of metal alloy materials is particularly notable[32-37]. In pavement engineering, AFM has been used to evaluate and characterize asphalt surface microstructures and micromechanical properties[38-41] study modified binders[42-44], explore the effects of ageing and recycling on asphalt adhesive properties[45-49], evaluate water damage[50] and binder-aggregate adhesion[51]. The potential of AFM for characterizing rock materials has also been explored, including studies on porosity and hydrocarbon reservoir rocks[52-54] and the identification and morphological characterization of microstructural elements in rocks, such as fractures[55-57]. The potential of AFM for characterizing rock materials has also been explored, including studies on porosity and hydrocarbon reservoir rocks[52-54] and the identification and morphological characterization of microstructural elements in rocks, such as fractures[55-57]. In geotechnics, Wang et al.[58] used SEM to obtain detailed information on the adhesion between aggregates and asphalt binder, advancing the understanding of the interaction mechanisms of these materials.

Scanning Electron Microscopy (SEM) has been widely employed in studies focused on qualitative morphological characterization at the microscale, owing to its capability to generate detailed images from secondary electrons. SEM enables the acquisition of high-resolution images of the morphology and microstructures present on sample surfaces[59]. Kuang et al.[60] employed SEM to analyze the microstructure of limestone and granite aggregates, focusing on the asphalt-aggregate interface, identifying deeper textures in limestone compared to granite. These results highlighted the greater roughness of limestone and its consequent influence on the aggregate's mechanical behaviour[60]. In geotechnics, Wang et al.[58] utilized SEM to obtain detailed image information regarding adhesion between aggregates and asphalt binder, contributing to a deeper understanding of these interaction mechanisms.

Although AFM and SEM techniques provide valuable information on roughness and microstructure, studies applying these advanced techniques to the characterization of mineral aggregates remain scarce. Due to the limited scanning area of AFM (areas smaller than $10 \times 10\ \mu m^2$), the combination of AFM and SEM emerges as a relevant approach for multiscale characterization of aggregate morphology[61]. This research aims to apply AFM and SEM techniques to characterize the surface roughness of mineral aggregates and compare their results with those obtained using the AIMS method. Based on the results, inconsistencies in the classification systems currently used in geotechnical engineering — which do not consider the micro- and nanoscale evaluation of aggregate morphology — will be identified and discussed. This study seeks to contribute to the advancement of morphological characterization methodologies and, consequently, to improving pavement performance and durability.

## 2. Experimental

### *2.1. Materials*

Two types of aggregates widely used in civil engineering of volcanic (surface crystallization) and plutonic (deep crystallization) origins, were selected for this study (Figure 1). The samples were collected from quarries located in the Rio Grande do Sul (RS) state, southern Brazil, exhibiting distinct morphological characteristics: one situated at the transition between the Serra Geral and Rio Jacuí Depression (SUL Quarry) and the other in the Lower Southern Rio Grande Plateau (MIN Quarry). Table 1 presents detailed information about the quarries, including their location, lithology, and petrographic characterisation of each aggregate.

### *2.2. Methods*

#### *2.2.1 AIMS roughness assessment*

The digital image processing of aggregates was performed using the Aggregate Imaging Measurement System (AIMS), as specified in the Brazilian technical standard DNIT 432/2020-


**Figure 1.** Photographic materials use for this study.

**Table 1.** Petrological characterisation of the aggregates used in the research.

| ID | Location | Lithology | Petrological characterization | | |
|---|---|---|---|---|---|
| | | | Texture | Structure | Mineralogy |
| SUL | Dilermando | Basalt | Aphanitic equigranular | No main foliation | 55% plagioclase; 35% pyroxene; 10% hematite and/or magnetite |
| MIN | Capão do Leão | Monzogranite | Phaneritic inequigranular | Magmatic flow foliation | 22% plagioclase; 45% pyroxene; 25% quartz; 3% biotite |

ME[16]. The tests were conducted at the Geotechnics/Pavement Laboratory of the Instituto Alberto Luiz Coimbra de Pós-Graduação e Pesquisa de Engenharia at the Universidade Federal do Rio de Janeiro (COPPE/UFRJ). The method followed three steps:

- Particle Preparation and Positioning: Aggregates were arranged in trays according to particle size. An initial verification was conducted to detect potential analytical acquisition errors.
- Image Acquisition: Using a high-resolution camera, grayscale images were captured for texture analysis.
- Image Processing: Morphological properties were quantified using specialized algorithms employing edge detection and segmentation techniques.

The surface roughness index via AIMS was calculated based on wavelet analysis, which evaluates surface irregularities (Equation 1).

$$Text.Sup._n = \frac{1}{3N}\sum_{t=1}^{3}\sum_{f=1}^{N}\left(D_{t,j}\left(x,y\right)\right)^2 \quad (1)$$

Where:

- D = decomposition function
- n = image decomposition level
- N = total number of coefficients in an image
- i = texture direction
- j = wavelet index
- x,y = location of coefficients in the domain

The resulting parameter, ranging from 0 to 1000, provides a quantitative measure of roughness, with higher values indicating rougher surfaces. The classification systems proposed by Al Rousan[62,63] and Ibiapina et al.[64] were adopted to interpret the results, as described in Table 2.

### 2.2.2. AFM roughness assessment

The micro- and nanoscale analysis using Atomic Force Microscopy (AFM) was performed with the Park Systems NX10 equipment at the Department of Physics at Universidade Federal de Santa Maria (UFSM). This technique was applied to complement the data obtained through AIMS, focusing on morphology, phase contrast, and amplitude. The methodology followed three experimental configurations:

- Operating Mode: Non-contact mode, suitable for preserving both the integrity of the rock material surface and the probe tip.
- Probes: PPPNCHR, with a resonance frequency of 330 kHz and a force constant of 42 N/m.
- Scanning Configuration: Scanning area of 10 × 10 µm, elevation height of 200 nm, resolution of 256 × 256 pixels, and a scanning rate of 0.35 Hz.

The acquired data were processed using the Gwyddion software, enabling the extraction of quantitative parameters of surface roughness at both the micro- and nanoscale levels. The integration of data obtained from AIMS and AFM aimed to evaluate the consistency between the proposed classification systems for rock aggregates, identifying potential incongruences and limitations in the existing systems.

### 2.2.3. Scanning Electron Microscopy (SEM)

The microstructural analysis performed by Scanning Electron Microscopy (SEM) used a JSM 6360 model, equipped with an energy dispersive X-ray spectroscopy (EDS) system, QUEST model, by ThermoSystem. The tests were conducted in the SEM Laboratory at UFSM.

The rock samples were subjected to a cleaning process to remove impurities before the analysis, following the recommendations of Nobre et al.[65] and Mallmann et al.[59]. The aggregates were then fixed on the sample holder using double-sided carbon adhesive tape. To ensure the necessary electrical conductivity for the analysis, the surfaces of the materials were coated with a nanometric gold layer via sputtering in a vacuum metal coater.

The images were obtained in topographic mode (Topo), which generates morphological contrasts based on the variation in the yield of secondary electrons emitted by the sample surfaces. The analyses were carried out at magnifications of 100x and 2000x, using an acceleration voltage of 20 kV and a beam with electric current of 20 nA. This procedure allowed the observation of the microstructural characteristics and the evaluation of the surface roughness of aggregates with high resolution.

**Table 2.** Threshold values established for surface texture classification according to the methodologies of Al Rousan et al.[63] and Ibiapina et al.[64].

| Classification System | Limit Values | | | | |
|---|---|---|---|---|---|
| Al Rousan et al.[63] | < 165 | 165 – 275 | 275 – 350 | 350 – 450 | > 460 |
| | Polished | Smooth | Low roughness | Moderate roughness | High roughness |
| Ibiapina et al.[64] | <260 | 260-440 | 440-600 | 600-825 | >825 |
| | Polished | Smooth | Low roughness | Moderate roughness | High roughness |

## 3. Results and Discussion

### *3.1. AIMS*

The roughness values obtained using the AIMS system are presented in Table 3, considering the classifications proposed by Al-Rousan[62] and Ibiapina et al.[64]. It can be observed that the volcanic rock (SUL) exhibited a higher roughness value (894.093) compared to the plutonic rock (MIN), which obtained a value of 66.32. Regardless of the classification used, both systems categorize the SUL material as “High Roughness” and the MIN as “Polished.”

**Table 3.** Values obtained for surface roughness by AIMS.

| ID | Value | Al Rousan et al.[63] | Ibiapina et al.[64]. |
|---|---|---|---|
| SUL | 894,093 | High Roughness | High Roughness |
| MIN | 66,32 | Polished | Polished |

Figure 2 shows the images captured by the AIMS system for surface texture, while Figure 3 represents a three-dimensional (3D) profile of the pixel distribution on the aggregate surface. The surface texture was analyzed based on the variation in pixel intensity captured by the camera, revealing that the SUL aggregate material has a higher density of peaks and valleys on the surface compared to the MIN rock. This difference can be observed through the color scale used, where rougher areas exhibit a heterogeneous color distribution. This behavior indicates that the SUL aggregate is likely to provide greater mechanical interaction in asphalt mixtures due to its high roughness, whereas the MIN material, with a smoother surface, may exhibit lower adhesion capacity.

The images obtained via AIMS do not always accurately reflect the actual characteristics of the analyzed aggregate. This occurs due to intrinsic limitations related to the camera focus during image capture, the photographed analysis area, the structure and granulation of the rock material, and

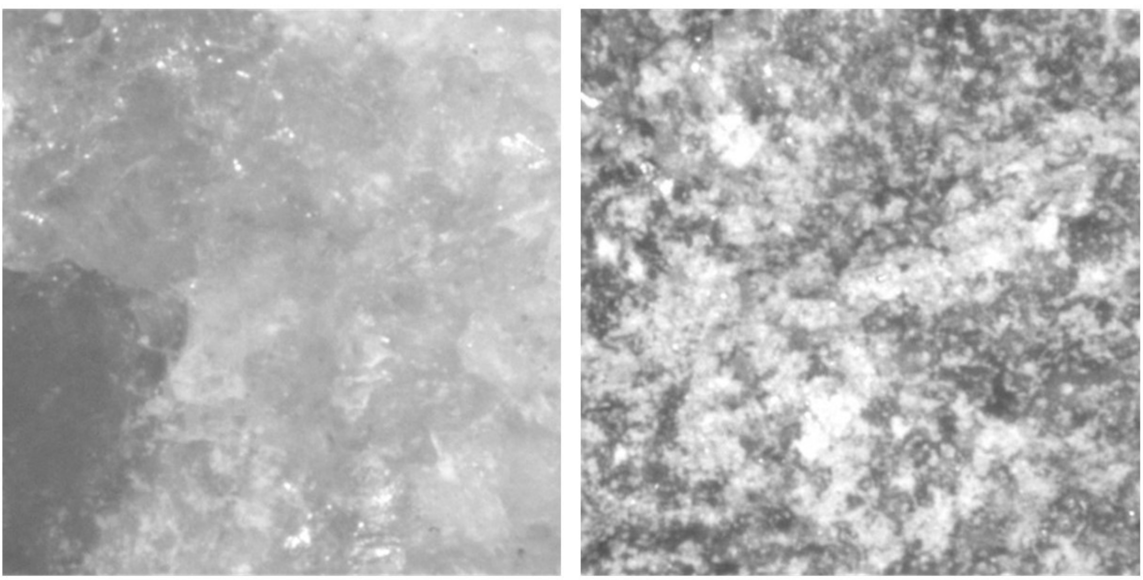

**a) MIN.** **b) SUL.**

**Figure 2.** Photographic record of pixels acquired by the AIMS system camera.

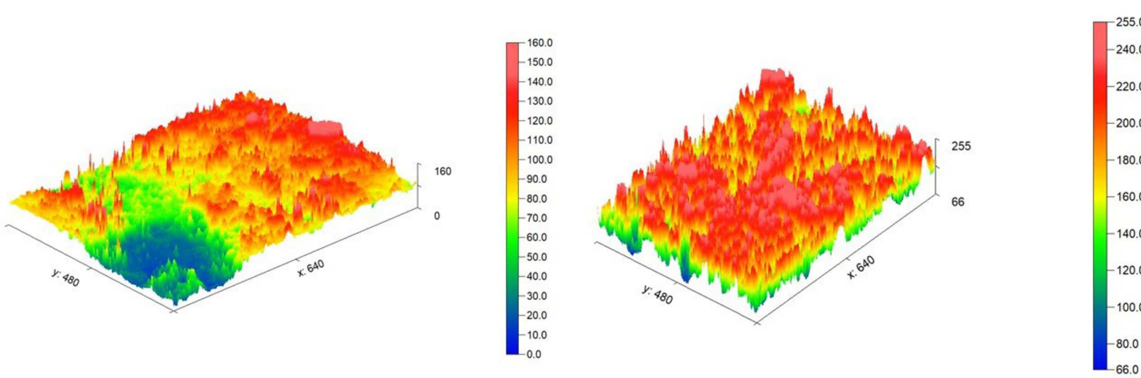


**a) MIN.** **b) SUL.**

**Figure 3.** Presentation of data obtained by AIMS.

subsequent processing, which involves the application of wavelet transformation.

The surface texture of the SUL aggregate is rougher than that of the MIN aggregate due to the geological origin differences between the rocks. The SUL rock, of volcanic origin and fine granulation, exhibits a more complex microstructural fabric with irregular morphology, whereas the MIN rock, of plutonic origin and coarser granulation, shows less morphological variation. The processing of data acquired via AIMS influences the representativeness of the results. In the case of the MIN rock, with its coarse texture, the analysis may be biased by isolated minerals since the camera focus can center on single phases, in addition to the wavelet transformation. This processing highlights the influence of dominant minerals, such as quartz and feldspar, resulting in texture values that are less representative of the aggregate. The fine-grained SUL rock allows the analysis to capture a more integrated combination of different minerals and microtextures present on the aggregate surface. This makes the obtained texture values more representative of the material's overall behavior. The 3D texture analysis reinforces this observation, with the SUL aggregate showing more numerous, intense, and irregular elevation peaks, while the MIN aggregate exhibits a predominantly homogeneous and flat surface.

### 3.2. AFM

AFM was used to obtain 3D roughness maps of the SUL and MIN samples in three different areas of each sample, providing a detailed and quantitative analysis of the topography. For this characterization, the following parameters were measured:

- Ra (Average Roughness): Represents the average difference between the height of a point and the mean surface level. It is obtained from the arithmetic mean of the height deviations of the surface relative to the sample plane[66-68]
- Rq (Root Mean Square Roughness): Calculates the standard deviation of the topography, representing the root mean square of the height deviations from the sample plane. This parameter is frequently used to evaluate surface texture.
- Rsk (Surface Skewness): Indicates the symmetry of the height distribution on the surface. A value close to zero suggests a smooth surface, positive values indicate a predominance of peaks, while negative values reflect a predominance of depressions.
- Rku (Surface Kurtosis): Reflects the concentration of heights around the mean value. Positive values suggest a more concentrated and sharp distribution, while negative values indicate greater dispersion of heights.

The results obtained for the analyzed samples are presented in Table 4.

Based on the results obtained, it is possible to describe the following points:

Ra e Rq (Average and Root Mean Square Roughness):

- The MIN sample showed higher Ra and Rq values in all analyzed areas, indicating greater irregularity and more pronounced surface height compared to the SUL sample.

**Table 4.** Statistical parameters generated as a result of AFM analysis.

| ID | Area | Ra | Rq | Rsk | Rku |
|---|---|---|---|---|---|
| SUL | 1 | 35,15 | 45,29 | 0,2606 | -0,425 |
| | 2 | 0,7809 | 0,9647 | -0,08454 | -0,7365 |
| | 3 | 13,55 | 20,36 | 1,203 | 2,014 |
| MIN | 1 | 137,3 | 170,1 | -0,054 | -0,6502 |
| | 2 | 109,8 | 131,5 | 0,5636 | -0,5393 |
| | 3 | 117,3 | 147,4 | -4,65 | -0,5388 |

- The SUL sample exhibited greater variability between the areas, with low values in some regions (Area 2), reflecting the microstructures heterogeneity.

Rsk (Skewness):

- In the SUL sample, Rsk values ranged from negative (-0.08454 in Area 2) to positive (1.203 in Area 3), indicating that the microtextures include both depressions and elevated peaks.
- The MIN sample had predominantly negative values, suggesting surfaces with more depressions than peaks or a more uniform height distribution.

Rku (Kurtosis):

- The kurtosis in the SUL sample showed values close to zero in some areas (indicating a normal height distribution) and positive in others, such as Area 3 (Rku = 2.014), suggesting a higher concentration of peaks on the surface.
- For the MIN sample, all Rku values were negative, indicating greater dispersion of heights and the absence of significant concentration around the mean value.

The fine granulation and heterogeneous composition of the SUL rock provided more representative AFM measurements, capturing detailed information about the different minerals that form its microstructures, even though they are quite heterogeneous between areas. This characteristic explains the greater variability in Rsk and Rku parameters across different areas. The coarse granulation and predominance of scanned areas containing only one mineral phase resulted in higher Ra and Rq values for the MIN rock. However, these results might suggest an apparent roughness influenced by the scanning of a single phase of the rock, reflecting a texture that is less representative of the aggregate.

Figures 4 and 5 present the three-dimensional surface roughness maps obtained by AFM for the SUL and MIN aggregates performed in three distinct areas of each sample. These diagrams allow a detailed visualization of the topographic differences influencing the roughness (Ra and Rq), skewness (Rsk), and kurtosis (Rku) values.

The SUL sample graphs indicate a more heterogeneous topography across the analyzed areas. In Area 1, a relatively homogeneous surface is observed, while in Area 2, more pronounced peaks appear frequently, aligning with the increased Ra and Rq values in this region. In Area 3, a profile with sharper peaks is noted, reflected in the higher positive skewness (Rsk = 1.203) and kurtosis exceeding 2.014, indicating the concentration of elevations in small

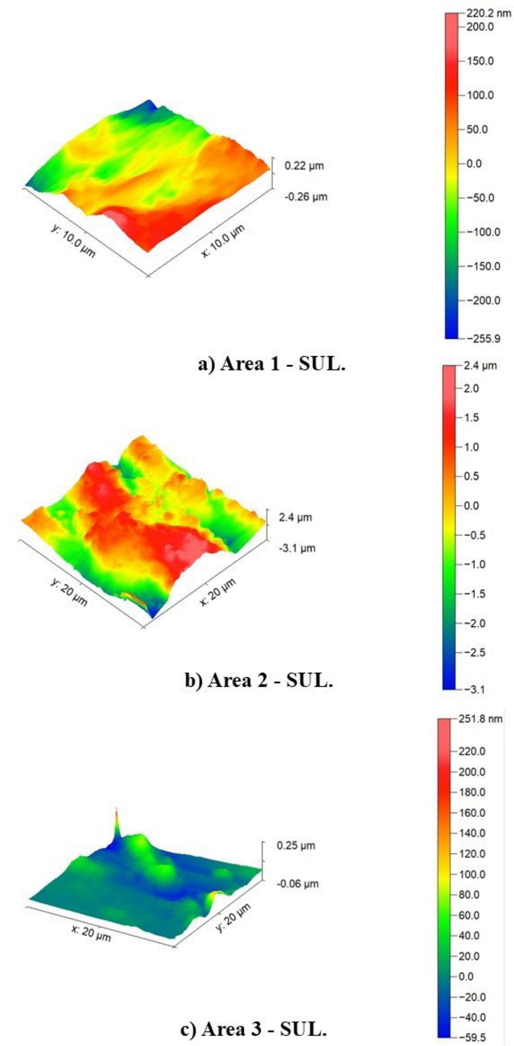


**Figure 4.** Surface roughness of SUL aggregate.

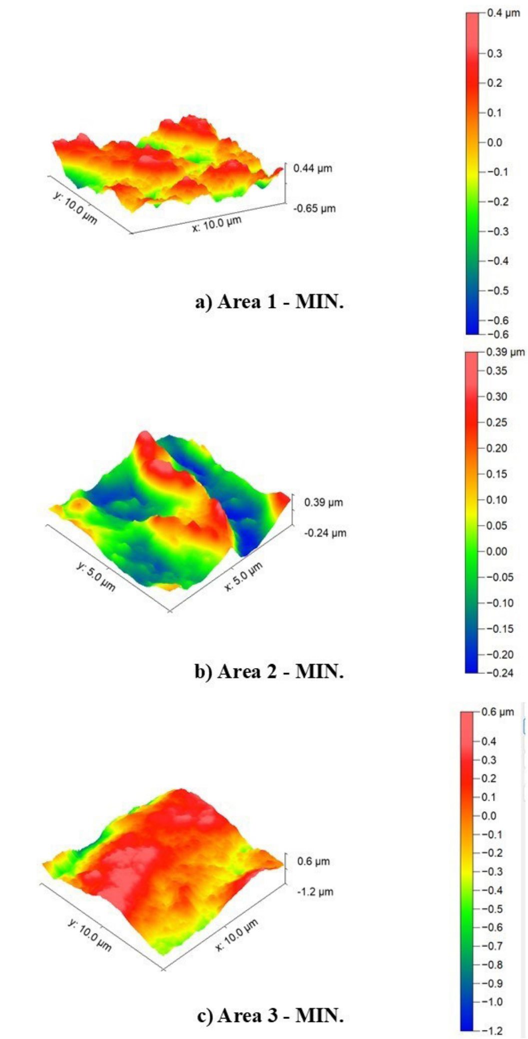


**Figure 5.** Surface roughness of MIN aggregate.

domains. The graphs of MIN aggregate suggest a more uniform texture across the three analyzed areas, although Area 3 shows significant variation with a prominent central peak, as indicated by the negative Rsk and an Rku value close to -0.5388. This topography confirms previously observed characteristics, where AFM detects isolated variations that can be attributed to the dominance of individual minerals in coarse-grained aggregates due to the scanning area limitations imposed by this characterization technique.

These 3D graphs demonstrate how the microstructures of aggregate surfaces, influenced by mineralogical composition and granulation, affect roughness parameters. In the case of SUL, the finer granulation allows the capture of multiple minerals, while in MIN, the more uniform texture is shaped by dominant minerals. The illustrated topography supports the discussion of roughness values and the limitations of the methods in representing the overall complexity of aggregate surfaces.

### 3.3. MEV

The secondary electron images generated by SEM of the aggregates from the SUL and MIN samples are shown in Figure 6.

At a 100x magnification, it is possible to observe differences in the morphology and distribution of mineral particles between the aggregates. The SUL aggregate (Figure 6A) shows a rougher surface, which is associated with the substantially fine (aphanitic) granulation of its matrix. In this type of microstructure, the constituent minerals are not visible to the naked eye but become perceptible under SEM, revealing a surface with relatively uniformly distributed roughness. The MIN aggregate (Figure 6B) exhibits coarse (phaneritic) granulation, characterized by minerals that are distinguishable to the naked eye and vary in size. This mineralogical feature results in areas with variable roughness: smooth plateaus associated with the surface of single minerals, such as quartz

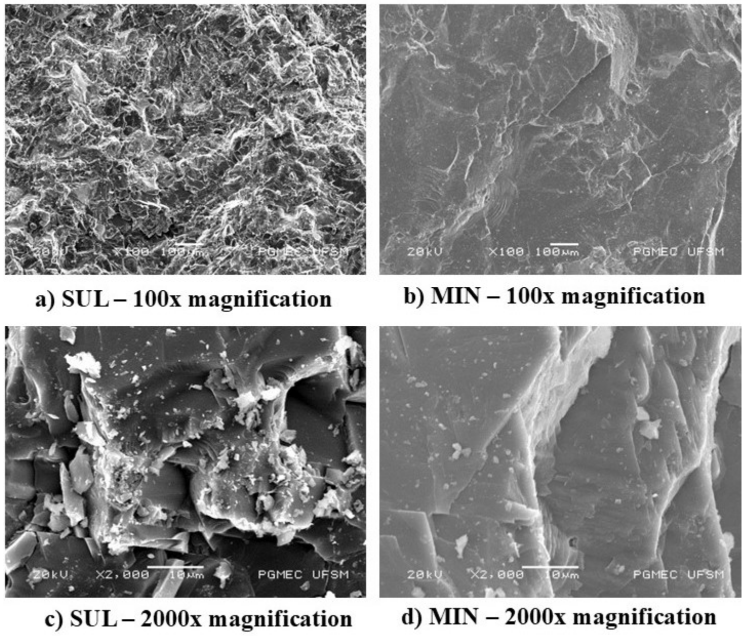


**Figura 6.** Secondary electron images of the SUL (A and C) and MIN (B and D) rock aggregates at 100 and 2000x magnification.

and feldspar (low roughness), and uneven regions with high roughness, usually related to cleavage planes, fractures, and crystal edges. Additionally, external influences, such as dust accumulation and other contaminants, were observed on the surfaces of both aggregates.

In 2000x magnification, the MIN aggregate (Figure 6D) maintains its heterogeneous surface roughness, with low-roughness areas interspersed with regions of pronounced unevenness, more clearly highlighting the cleavage planes and fractures of the minerals. This observation reinforces the relationship between roughness and mineral grain size, where minerals more susceptible to cleavage and fracture exhibit significant morphological irregularities along crystal edges. The SUL aggregate (Figure 6C), at a 2000x magnification, revealed cleavage planes and mineral fractures, patterns that were not observable at lower magnifications.

### *3.4. Critical analysis and discussion between AIMS, AFM and SEM results*

Based on the results obtained from the AIMS, AFM, and SEM tests, it is evident that further investigation is needed regarding the microstructure and fine-grained materials in the classification systems currently used in geotechnical engineering, highlighting the methodological limitations of AIMS and the relevance of AFM and SEM as complementary approaches for material characterization at different scales.

The AIMS results reveal that, according to the classification systems of Al-Rousan[62] and Ibiapina et al.[64], the volcanic aggregate (SUL) exhibits high roughness, while the plutonic aggregate (MIN) is classified as polished. Although these classifications are useful for general comparisons, they do not adequately represent the microstructures of the aggregates. AIMS, relying on two-dimensional images and wavelet processing, is limited by the representativeness of the captured areas, as with other techniques. However, this limitation is particularly evident in coarse-textured rocks, such as the MIN aggregate, where the captured image predominantly reflects the characteristics of coarse minerals, overlooking variations that may significantly impact the material's mechanical behavior. Moreover, the output provided by the AIMS test is made available only after image processing, which prevents the wavelet-based texture analysis technique from being reliably reapplied to the other analyses performed in this study. This limitation, to some extent, hinders the possibility of conducting comparisons under the same experimental conditions. Additionally, AIMS has inherent limitations in image acquisition, as the fixed camera with automatic focus does not ensure sufficient image quality for representativity — regardless of the subsequent processing method. Another factor restricting the use of AIMS is the limited availability of equipment compared to SEM and AFM, making AIMS a less accessible technique.

The AFM results provide a more detailed view of surface texture, with quantitative parameters such as Ra, Rq, Rsk, and Rku, as well as high-resolution morphological models. These parameters reveal nuances of roughness not captured by AIMS. For the SUL aggregate, AFM indicated a more heterogeneous surface (at the micro and nanometric scale) with more pronounced peaks, characteristics that corroborate the high roughness classification obtained by AIMS, but with greater precision. For the MIN aggregate, AFM demonstrated that, despite appearing to have a more uniform surface, variations exist that suggest the presence of microstructures not captured by AIMS due to the method's limited resolution.

Complementing these analyses, the SEM results provided qualitative characterization of the surfaces at the micro-scale, offering insights into the aggregate morphology. For the SUL aggregate, images obtained at 100x and 2000x magnifications revealed a homogeneous surface, with roughness linked to the fine (aphanitic) texture of the parent rock. This roughness is evenly distributed in bulk analyses but begins to highlight mineral-dependent features, such as cleavages and fractures, when observed at the micro-scale. In the MIN aggregate, SEM images revealed a surface with smooth plateaus associated with minerals and regions of pronounced unevenness related to crystal edges. This morphology is emphasized at the 2000x magnification, where mineral cleavages and fractures become more evident as factors contributing to roughness, which are not detected by AIMS and are corroborated by AFM data.

These comparisons emphasize the importance of integrating methods such as SEM and AFM to complement AIMS analyses. Although AIMS is considered an effective method in geotechnics for initial macroscopic evaluation, it lacks the resolution needed to consider microstructures and roughness variations related to micro and nanometric granulation, which may impact properties such as the adhesion of binders to rock aggregates. AFM provides micro and nanoscale analyses with effective roughness values, but it evaluates more restricted surface areas compared to the other techniques, while SEM offers detailed qualitative characterization at the micro-scale. Together, these methods are complementary and essential for a comprehensive understanding of the surface roughness of aggregates. The combined use of these techniques provides a multi-scale (bulk, micro, and nano) view of the aggregate surfaces, allowing the identification of critical properties that directly influence the adhesion to asphalt binders and, consequently, the mechanical performance of asphalt mixtures. This integrated approach highlights the limitations of classification systems based solely on AIMS and represents a contribution to improving aggregate selection criteria and, consequently, the performance and durability of paved structures. Therefore, this study emphasizes the need to revise and enhance the classification systems currently in use, integrating advanced characterization techniques such as AFM and SEM[69,70]. The combination of these methods provides a more robust and representative characterization of aggregate surfaces, with direct implications for pavement engineering and other areas of geotechnical engineering.

## 4. Conclusions

The results of this study highlighted limitations in the aggregate roughness classification systems currently used in geotechnical engineering, with a focus on the AIMS method. Although widely adopted, AIMS is an optical technique limited to the bulk scale and is insufficient to capture the complexity of microstructures, particularly in coarse-textured rocks such as the MIN aggregate. The analysis was influenced by coarse minerals, compromising the representativeness of the obtained data and omitting fine features that can only be analyzed at the micro and nanometric scales. The combined use of SEM and AFM offers a complementary approach for studying the roughness of rock aggregates. SEM enabled detailed qualitative characterization at the micro-scale, revealing morphological variations related to texture and crystal edges, with smooth plateaus and unevenness in fractures and cleavages. AFM provided measurements at micro and nano scales, generating three-dimensional maps and quantitative parameters (Ra, Rq, Rsk, Rku) not generated by traditional methods. Although SEM lacks resolution for nanometric-scale analysis, it generates three-dimensional results. Conversely, while AFM can detect nanometric roughness, standardizing it for micrometric-scale analysis would lead to the loss of relevant data for roughness assessment.

This study contributes to the discussion on rock aggregate characterization methodologies for pavement applications by proposing the integration of micro and nano-scale analyses as new dimensions in aggregate evaluation. It is important to emphasize that the image acquisition process underlying roughness pattern analysis must be representative in both scale and content to allow for accurate processing, regardless of the technique employed (e.g., wavelet, Ra, Rq, Rsk, Rku, or others not considered in this study). This study highlights the need to update the currently adopted standards for classifying aggregate roughness, which are primarily based on data obtained through imaging techniques. These factors are relevant for adhesion to asphalt binders, and previous bulk-based approaches were insufficient to analyze them. The use of techniques such as SEM and AFM can provide valuable insights for developing more refined classification systems that align with the performance and durability requirements of advanced pavement structures.

## 5. Acknowledgments

The authors would like to thank CAPES for funding the research and providing research scholarships, the COPPE Lab at Universidade Federal do Rio de Janeiro, and the Laboratory of Magnetism and Magnetic Materials (LMMM) and the Scanning Electron Microscopy (SEM) Laboratory at UFSM for enabling the execution of the experiments.

## 6. References

1. Přikryl R. Geomaterials as construction aggregates: a state-of-the-art. Bull Eng Geol Environ. 2021;80(12):8831-45. http://doi.org/10.1007/s10064-021-02488-9.
2. Stakston AD, Bahia HU. The effect of fine aggregate angularity, asphalt content and performance graded asphalts on hot mix asphalt performance. Madison: Univesity of Wisconsin; 2003. Wisconsin Highway Research Program.
3. Diógenes LM, Bessa IS, Branco VTFC, Mahmoud E. The influence of stone crushing processes on aggregate shape properties. Road Mater Pavement Des. 2018;20(4):877-94. https://doi.org/10.1080/14680629.2017.1422792.
4. Diógenes L, Maia R, Bessa I, Branco VC, Neto JN, Silva F. The influence of crushing processes and mineralogy of aggregates on their shape properties and susceptibility to degradation. Constr Build Mater. 2021;284:122745. http://doi.org/10.1016/j.conbuildmat.2021.122745.
5. Cui PD, Wu SP, Xiao Y, Xu HQ. Effect of coarse aggregate morphologies on the hydrodynamic pressure– resulted moisture susceptibility of asphalt mixtures. J Mater Civ Eng. 2020;32(11):04020343. http://doi.org/10.1061/(ASCE)MT.1943-5533.0003446.
6. Gong F, Zhou X, You Z, Liu Y, Chen S. Using discrete element models to track movement of coarse aggregates du ring compaction of asphalt mixture. Constr Build Mater. 2018;189:338-51. http://doi.org/10.1016/j.conbuildmat.2018.08.133.
7. Du S, Wu J, Alshareedah O, Shi X. Nanotechnology in cement-based materials: a review of durability, modeling, and advanced characterization. Nanomaterials (Basel). 2019;9(9):1213. http://doi.org/10.3390/nano9091213. PMid:31466289.

8. Nobre AG, Martínez JAE, Florêncio O. Mineral nanotechnology in circular economy. In: Iano Y, Saotome O, Kemper G, Mendes de Seixas AC, Gomes de Oliveira G, editors. 6th Brazilian Technology Symposium (BTSym'20). BTSym 2020. Smart Innovation, Systems and Technologies; 2020; Cham. Proceedings. Cham: Springer International Publishing; 2020. v. 233, p. 220-6. http://doi.org/10.1007/978-3-030-75680-2_26.
9. Bessa IS. Avaliação do processamento digital de imagens como ferramenta para caracterização de agregados e misturas asfálticas [dissertation]. Fortaleza: Departamento de Transportes, Universidade Federal do Ceará; 2012.
10. Greer M, Heitzman M. Evaluation of the AIMS2 and micro-deval to characte rize aggregate friction properties. USA: Auburn University; 2017. NCAT Report 17-02.
11. Castelo Branco VTF, Masad E, Little DN, Soares JB, Motta LMG. Caracterização de forma, angularidade e textura de agregado de brita granítica e escórias de aciária usando o Aggregate Imaging System (AIMS). In: XX Congresso de Pesquisa e Ensino em Transportes; 2006; Brasília, DF. Anais. Rio de Janeiro: ANPET; 2006.
12. Al-Rousan T, Masad E, Myers L, Speigelman C. New methodology for shape classification of aggregates. Transp Res Rec. 2005;1913(193):11-23. http://doi.org/10.1177/0361198105191300102.
13. Wang F, Xiao Y, Cui P, Ma T, Kuang D. Effect of aggregate morphologies and compaction methods on the skeleton structures in asphalt mixtures. Constr Build Mater. 2020;263:120220. http://doi.org/10.1016/j.conbuildmat.2020.120220.
14. Ceccato HD. Avaliação e caracterização do comportamento geomecânico de agrega dos oriundos de jazidas da região sudeste do Rio Grande do Sul e Santa Catarina [dissertation]. Santa Maria: Universidade Federal de Santa Maria; 2021.
15. Skibsted J, Hall C. Characterization of cement minerals, cements and their reaction products at the atomic and nano scale. Cement Concr Res. 2008;38(2):205-25. http://doi.org/10.1016/j.cemconres.2007.09.010.
16. DNIT: Departamento Nacional de Infraestrutura de Transportes. DNIT 432/2020. Determinação das propriedades de forma por meio do processamento digital de imagens (PDI). Brasília: DNIT; 2020.
17. Luo Z, Li W, Wang K, Shah SP. Research progress in advanced nanomechanical characterization of cement-based materials. Cement Concr Compos. 2018;94:277-95. http://doi.org/10.1016/j.cemconcomp.2018.09.016.
18. Chen Y, Hou Y, Ji X, Zou H, Sai C, Chen B. Characterization of surface mechanical properties of various aggregates from micro scale using AFM. Constr Build Mater. 2021;286:122847. http://doi.org/10.1016/j.conbuildmat.2021.122847.
19. Binning G, Quate CF, Gerber C. Atomic force microscope. Phys Rev Lett. 1986;56(9):930-3. http://doi.org/10.1103/PhysRevLett.56.930. PMid:10033323.
20. Bhushan B, Kasai T, Nguyen CV, Meyyappan M. Multiwalled carbon nanotube AFM probes for surface characterization of micro/nanostructures. Microsyst Technol. 2004;10(8):633-9. http://doi.org/10.1007/s00542-004-0489-x.
21. Stipp SLS, Eggleston CM, Nielsen BS. Calcite surface structure observed at microtopographic and molecular scales with atomic force microscopy (AFM). Geochim Cosmochim Acta. 1994;58(14):3023-33. http://doi.org/10.1016/0016-7037(94)90176-7.
22. Dove PM, Platt FM. Compatible real-time rates of mineral dissolution by Atomic Force Microscopy (AFM). Chem Geol. 1996;127(4):331-8. http://doi.org/10.1016/0009-2541(95)00127-1.
23. Yong L, Yang J, Pan Z, Tang W. Nanoscale pore structure and mechanical property analysis of coal: an insight combining AFM and SEM images. Fuel. 2020;260:116352. http://doi.org/10.1016/j.fuel.2019.116352.
24. Dobe R, Das A, Mukherjee R, Gupta S. Evaluation of grain boundaries as percolation pathways in quartz-rich continental crust using Atomic Force Microscopy. Sci Rep. 2021;11(1):9831. http://doi.org/10.1038/s41598-021-89250-z. PMid:33972600.
25. Wang Y, Zhang H. Influence of asphalt microstructure to its high and low temperature performance based on atomic force microscope (AFM). Constr Build Mater. 2021;267:120998. http://doi.org/10.1016/j.conbuildmat.2020.120998.
26. Das S, Chaudhari AK, Singh VK, Dwivedy AK, Dubey NK. *Angelica archangelica* essential oil loaded chitosan nanoemulsion as edible coating for preservation of table grape fruit against *Botrytis cinerea* contamination and storage quality deterioration. Postharvest Biol Technol. 2023;205:112482. http://doi.org/10.1016/j.postharvbio.2023.112482.
27. Matos RS, Pinto EP, Pires MA, Ramos GQ, Talu S, Lima LS, et al. Evaluating the roughness dynamics of kefir biofilms grown on Amazon cupuaçu juice: a monofractal and multifractal approach. Microscopy (Oxf). 2024;73(1):55-65. http://doi.org/10.1093/jmicro/dfad040. PMid:37540558.
28. Monteiro VF, Natal AMD, Soledade LEB, Longo E. Morphological analysis of polymers on hair fibers by SEM and AFM. Mater Res. 2003;6(4):501-6. http://doi.org/10.1590/S1516-14392003000400013.
29. Lee G-J, Park KH, Park YG, Park HK. A quantitative AFM analysis of nano-scale surface roughness in various orthodontic brackets. Micron. 2010;41(7):775-82. http://doi.org/10.1016/j.micron.2010.05.013. PMid:20646928.
30. Farias ACM, Medeiros JTN, Alves SM. Micro and nanometric wear evaluation of metal discs used on determination of biodiesel fuel lubricity. Mater Res. 2014;17(Suppl 1):89-99. http://doi.org/10.1590/S1516-14392014005000101.
31. Stryhalski J, Fontana LC, Odorczyk MF, Scholtz JS, Sagás JC, Recco AAC. Pulsed bias effect on crystallinity and nano-roughness of Ti6Al4V-N films deposited by grid assisted magnetron sputtering system. Mater Res. 2014;17(6):1545-9. http://doi.org/10.1590/1516-1439.271314.
32. Pascoal CVP, Silva GB, Silva DS, Salomão FCCS, Barris EB, Vasques EB, et al. Study of protic ionic liquids as sustained corrosion inhibitors for mild steel in saline solution with acidic pH and temperature variations. Mater Res. 2024;27(Suppl 1):e20240047. https://doi.org/10.1590/1980-5373-MR-2024-0047.
33. Moura MJS, Vasques RB, Levy MM, Magalhães SJM, Pascoal CVP, Almeida-Neto FWQ, et al. Study of the efficiency of the amino acid l-histidine as a corrosion inhibitor of 1018 carbon steel in saline solution without and with $CO_2$ saturation. Mater Res. 2024;27(Suppl 1):e20240135. http://doi.org/10.1590/1980-5373-MR-2024-0135.
34. Souza MA, Lima MCM, Escada ALA, Pimentel BNAS, Vergani CE, Sabino RM, et al. Surface modification of the Ti25Ta25Nb3Sn alloy and its influence on the cell and bacteria adhesion-in vitro studies. Mater Res. 2023;26:e20230113. http://doi.org/10.1590/1980-5373-mr-2023-0113.
35. Madureira HP, Monção RM, Silva AA, Hidalgo AA, Vega ML, Feitor MC, et al. Study of the optoelectronic properties of titanium nitride thin films deposited on glass by reactive sputtering in the cathodic cage. Mater Res. 2023;26:e20230187. http://doi.org/10.1590/1980-5373-mr-2023-0187.
36. Sridhar S, Marichamy S, Subbiah R. Evaluation of abrasive wearrate and machining behaviors of synthesized nitinol composite. Mater Res. 2022;25:e20220161. http://doi.org/10.1590/1980-5373-mr-2022-0161.
37. Fischer RR, Recco AAC, Garzón CM. Mechanical preparation procedure for characterizing by EBSD the crystallographic orientation in surface layers of austenitic stainless steels plasma nitrided. Mater Res. 2021;24(5):e20210034. http://doi.org/10.1590/1980-5373-mr-2021-0034.
38. Guo M, Huang Y, Wang L, Yu J, Hou Y. Using atomic force microscopy and molecular dynamics simulation to investigate the asphalt micro properties. Int J Pavement Res Technol. 2018;11(4):321-6. http://doi.org/10.1016/j.ijprt.2017.09.017.

39. Yu X, Burnham NA, Tao M. Surface microstructure of bitumen characterized by atomic force microscopy. Adv Colloid Interface Sci. 2015;218:17-33. http://doi.org/10.1016/j.cis.2015.01.003. PMid:25678270.
40. Chen Y, Li H, Yu W, Dong X, He G, Wu T. Characterization of the micromorphology of asphalt surfaces using atomic force microscopy. Constr Build Mater. 2023;401:132845. http://doi.org/10.1016/j.conbuildmat.2023.132845.
41. Sun E, Zhao Y, Wang G. Analysis of nanoscale evolution features of microstructure of asphalt based on atomic force microscopy. Constr Build Mater. 2023;409:133958. http://doi.org/10.1016/j.conbuildmat.2023.133958.
42. Gong M, Zhu H, Pauli T, Yang J, Wei J, Yao Z. Evaluation of bio-binder modified asphalt's adhesion behavior using sessile drop device and atomic force microscopy. Constr Build Mater. 2017;145:42-51. http://doi.org/10.1016/j.conbuildmat.2017.03.114.
43. Chen B, Shen J, Wang W. Study on macro and micro properties of SBS-T/CRM dry mixed composite modified asphalt. Constr Build Mater. 2024;437:136752. http://doi.org/10.1016/j.conbuildmat.2024.136752.
44. Li Z, Chen Y, Guo T, Jia Q, Wang J, Jin L. Performance and mechanism analysis of waste edible oil recycled asphalt. Ecotoxicol Environ Saf. 2024;287:117242. http://doi.org/10.1016/j.ecoenv.2024.117242. PMid:39471668.
45. Rebelo LM, Sousa JS, Abreu AS, Baroni MPMA, Alencar AEV, Soares AS, et al. Aging of asphaltic binders investigated with atomic force microscopy. Fuel. 2014;117:15-25. http://doi.org/10.1016/j.fuel.2013.09.018.
46. Wang M, Liu L. Investigation of microscale aging behavior of asphalt binders using atomic force microscopy. Constr Build Mater. 2017;135:411-9. http://doi.org/10.1016/j.conbuildmat.2016.12.180.
47. Chen A, Liu G, Zhao Y, Li J, Pan Y, Zhou J. Research on the aging and rejuvenation mechanisms of asphalt using atomic force microscopy. Constr Build Mater. 2018;167:177-84. http://doi.org/10.1016/j.conbuildmat.2018.02.008.
48. Li B, Guo S, Chen X, Nan X, Chen Z, Li D, et al. Nanoscale study on adhesion performance and aging degree prediction of warm mix asphalt under UV aging condition. Case Studies in Construction Materials. 2023;18:e02143. http://doi.org/10.1016/j.cscm.2023.e02143.
49. Sun E, Zhao Y, Cai R. Characterization of microstructural evolution of asphalt due to water damage using atomic force microscopy. Constr Build Mater. 2024;438:137175. http://doi.org/10.1016/j.conbuildmat.2024.137175.
50. Sun E, Cai R, Zhao Y, Fu G, Che T. Microstructural and micromechanical evolution features of asphalt with aging: an atomic force microscopy study. Constr Build Mater. 2024;441:137518. http://doi.org/10.1016/j.conbuildmat.2024.137518.
51. Cui Y, Geng K, Zhou Q, Zhang S. Research on the adhesion between warm mix recycled asphalt and aggregates at macro and micro scales. Constr Build Mater. 2024;455:139076. http://doi.org/10.1016/j.conbuildmat.2024.139076.
52. Cohen AD, Bailey AM, Myrick ML, Doescher M, Friese WC, Thibodeaux S, et al. Applications of atomic force microscopy to study of artificially coalified peats. In: 15th Annual Meeting of the Society for Organic Petrology; 1998; Halifax, Canada. Abstracts. Alexandria: The Society for Organic Petrology; 1998. p. 23-6.
53. Yao S, Jiao K, Zhang K, Hu W, Ding H, Li M, et al. An atomic force microscopy study of coal nanopore structure. Chin Sci Bull. 2011;56(25):2706-12. http://doi.org/10.1007/s11434-011-4623-8.
54. Liu Y, Zou G, She J, Deng B, Yang H. Nanoscale physical parameters of source rocks identified by atomic force microscopy: a review. Geol J. 2022;57(10):4345-56. http://doi.org/10.1002/gj.4548.
55. Siman-Tov S, Aharonov E, Sagy A, Emmanuel S. Nanograins form carbonate fault mirrors. Geology. 2013;41(6):703-6. http://doi.org/10.1130/G34087.1.
56. Voigtländer A, Leith K, Krautblatter M. Subcritical crack growth and progressive failure in Carrara marble under wet and dry conditions. J Geophys Res Solid Earth. 2018;123(5):3780-98. http://doi.org/10.1029/2017JB014956.
57. Gurgurewicz J, Mège D, Skiscim M, Pers J. Nanotopographic characterization of microfractures in rocks by Atomic Force Microscopy. J Struct Geol. 2019;124:70-80. http://doi.org/10.1016/j.jsg.2019.04.010.
58. Wang S, Du F, Alghamdi S, Feng J, Chen F, Wang Z, et al. Effects of loading rates on interfacial adhesion between aggregates and asphalt binders. Constr Build Mater. 2023;408:133454. http://doi.org/10.1016/j.conbuildmat.2023.133454.
59. Mallmann LL, Nobre AG, Chemale F Jr, Netto RG, Paim PSG, Oliveira RFG. Unveiling CCS Potential of the Rio Bonito Formation, Paraná Basin, southern Brazil: the dawsonite discovery. Mineral Petrol. 2024;118(4):501-12. http://doi.org/10.1007/s00710-024-00871-4.
60. Kuang D, Zhang B, Jiao Y, Fang J, Chen H, Wang L. Impact of particle morphology on aggregate-asphalt interface behavior. Constr Build Mater. 2017;132:142-9. http://doi.org/10.1016/j.conbuildmat.2016.11.132.
61. Russell PE, Thornton DBJ. SEM and AFM: complementary techniques for high resolution surface investigations. New York: Veeco Instruments Inc., 2001. 12 p.
62. Al Rousan TM. Characterization of aggregate shape properties using a computer automated system. [dissertation]. College Station: Texas A&M Univeristy; 2004.
63. Al Rousan T, Masad E, Myers L, Speigelman C. New methodology for shape classification of aggregates. Transp Res Rec. 2005;1913(193):11-23. http://doi.org/10.1177/0361198105191300102.
64. Ibiapina DS, Diógenes LM, Castelo Branco VTF, Freitas SM, Motta LMG, Diógenes DF. Análise estatística da qualidade das medidas das propriedades de forma de agregados com o uso do processamento digital de imagens (PDI). Transportes. 2020;28(5):1-12. https://doi.org/10.14295/transportes.v28i1.1865.
65. Nobre AG, Andrade FRD, Salazar-Naranjo AF, Rigue JN, Silva RB, Vlach, SRF, Ando, RA. Electrical resistance evolution of graphite and talc geological heterostructures under progressive metamorphism. C. 2023;9(3):75. https://doi.org/10.3390/c9030075.
66. Abouletta OB, Madl J. Surface roughness prediction based on cutting parameters and tool vibrations in turning operations. J Mater Process Technol. 2001;118(1-3):269-77. http://doi.org/10.1016/S0924-0136(01)00959-1.
67. Huang HH, Ho CT, Lee TH, Lee TL, Liao KK, Chen FL. Effect of surface roughness of ground titanium on initial cell adhesion. Biomol Eng. 2004;21(3-5):93-7. http://doi.org/10.1016/j.bioeng.2004.05.001. PMid:15567102.
68. Chang WR, Kim IJ, Manning DP, Bunterngchit Y. The role of surface roughness in the measurement of slipperiness. Ergonomics. 2001;44(13):1200-16. http://doi.org/10.1080/00140130110085565. PMid:11794764.
69. Nobre AG, da Silva LPN, Andrade FRD. Graphene geology and the fourth industrial revolution. In: Iano Y, Saotome O, Kemper Vásquez GL, Cotrim Pezzuto C, Arthur R, Gomes de Oliveira G, editors. 7th Brazilian Technology Symposium (BTSym'21). BTSym 2021. Smart Innovation, Systems and Technologies; 2022; Cham. Proceedings. Cham: Springer; 2022. v. 207, p. 342-8. http://doi.org/10.1007/978-3-031-04435-9_34.
70. Nobre AG, Salazar-Naranjo AF, Andrade FRD, Vlach SRF, Ando RA. Simulation of geological graphene genesis by the piston-cylinder apparatus. Materia (Rio J). 2022;27(4):e20220122. http://doi.org/10.1590/1517-7076-rmat-2022-0122.

## Data Availability

The entire dataset supporting the results of this study was published in the article itself.